ELSEVIER

Ceramics International 31 (2005) 883–888

CERAMICS INTERNATIONAL

www.elsevier.com/locate/ceramint

Microwave-assisted synthesis of nanocrystalline MWO_4 (M: Ca, Ni) via water-based citrate complex precursor

Jeong Ho Ryu[a,*], Jong-Won Yoon[a], Chang Sung Lim[b], Won-Chun Oh[b], Kwang Bo Shim[a]

[a]*Department of Ceramic Engineering, CPRC, Hanyang University, Seoul 133-791, Korea*
[b]*Department of Adv. Mat. Sci. and Eng., CPRC, Hanseo University, Seosan 356-706, Korea*

Received 19 July 2004; received in revised form 23 August 2004; accepted 24 September 2004
Available online 12 January 2005

Abstract

Nano-sized MWO_4 (M: Ca, Ni) powders, which have scheelite and wolframite type structure, were successfully synthesized at low temperatures by a modified citrate complex method assisted by microwave irradiation. The citrate complex precursors were heat-treated at temperatures from 300 to 500 °C for 3 h. Crystallization of the $CaWO_4$ and $NiWO_4$ nano-sized powders were detected at 300 and 350 °C, respectively, and completed at a temperature of 400 °C. Most of the $CaWO_4$ and $NiWO_4$ powders heat-treated between 350 and 450 °C showed primarily spherical and homogeneous morphology. The average crystallite sizes of $CaWO_4$ and $NiWO_4$ were between 12 and 35 nm and between 14 and 29 nm, respectively, showing an ordinary tendency to grow with temperature.

Keywords: MWO_4 (M: Ca, Ni); Citrate complex; Microwave irradiation

1. Introduction

$CaWO_4$ and $NiWO_4$ are important inorganic materials of the metal tungstate families that have high application potential in various fields, such as in photoluminescence [1], microwave applications [2], optical fibers [3], scintillator materials [4], humidity sensors [5], magnetic properties [6] and catalysis [7]. Metal tungstate of relatively large bivalent cations (MWO_4, ionic radius > 0.99 Å, M: Ca, Ba, Pb, Sr) exist in the so-called scheelite structure form (scheelite: $CaWO_4$), where the tungsten atom adopts tetrahedral coordination. Tungstates of smaller bivalent cations (MWO_4, ionic radius < 0.77 Å: M: Fe, Mn, Ni, Mg), however, belong to the wolframite structure (wolframite: (Fe, Mn)WO_4), where the tungsten atom adopts an overall six-fold coordination [8].

Most previous approaches to the preparation of these families of compounds need high-temperature and harsh reaction conditions, such as the Czochralski method [9], reaction in aqueous medium followed by heating of the precipitates [10], the conventional solid-state method [11] and the hydro-thermal reaction over an extensive period [12]. However, metal tungstate particles prepared by these processes are relatively large with inhomogeneous morphology and composition. Inhomogeneous compounds of $CaWO_4$ and $NiWO_4$ might be easily formed because the WO_3 has a tendency to vaporize at high temperatures [13], and the temperature for the solid-state reaction is relatively high, almost above 1000 °C for 24 h [11].

These problems could be solved by applying advanced wet chemical methods. Polymerized complex method as a modified Pechini method [14], where several metal ions in a solution could be first chelated to form metal complexes and then polymerized to form a gel, seems to be most suitable among chemical solution processes, because rigidly fixed cations are homogeneously dispersed in the polymer network and have few chances to segregate even

* Corresponding author. Present address: 17 Haengdang-dong, Seongdong-gu, Seoul 133-791, Korea. Tel.: +82 2 2290 0543; fax: +82 2 2299 2884.
E-mail address: jimihen@ihanyang.ac.kr (J.H. Ryu).

0272-8842/$30.00
doi:10.1016/j.ceramint.2004.09.015

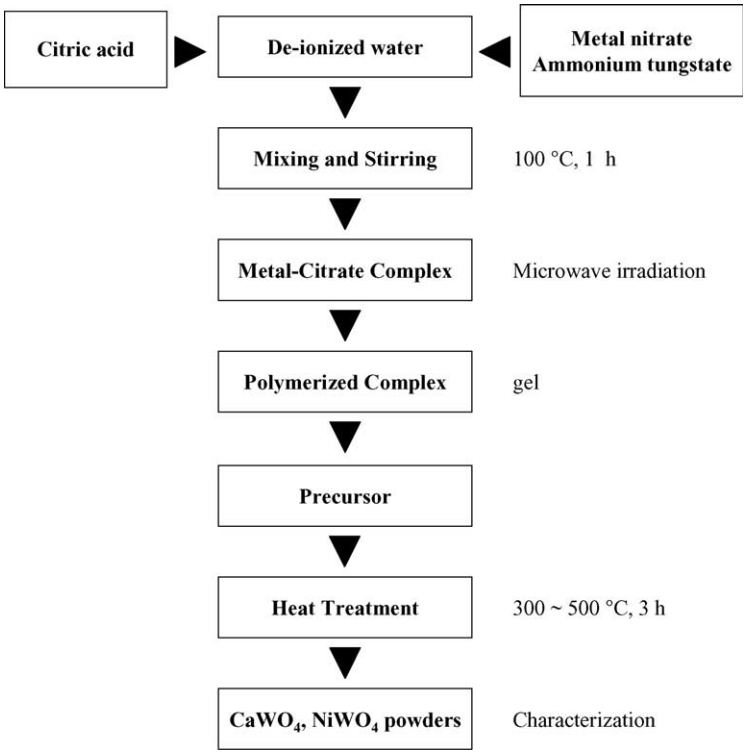

Fig. 1. Flow chart for the synthesis of nano-sized $CaWO_4$ and $NiWO_4$ powders by the modified citrate complex method under microwave irradiation.

during pyrolysis. This method has already been successfully used to prepare highly pure powders of various double oxides such as $BaTiO_3$ [15], Y_6WO_{12} [16], mixed-cation oxides [17] and even for various superconductors [18] with multiple cationic compositions. However, in spite of the many advantages of the polymeric complex method, the weakness of this method is the difficulty of the effective removal of the large amount of organic substances. Based on this consideration, the citrate complex method as another chemical solution process was tried in this work for the synthesis of nanocrystalline $CaWO_4$ and $NiWO_4$ powders. In this process, metal citrate complexes without a network structure are formed from water instead of ethylene glycol.

On the other hand, microwave irradiation as a heating source has been found and developed for a number of applications in chemical and ceramic processing [19–21]. Compared with the usual methods, microwave synthesis has the advantages of shortening the reaction time, giving products with small particle size, narrow particle size distribution and high purity. Jansen et al. [19] suggested that these advantages could be attributed to fast homogeneous nucleation and easy dissolution of the gel.

In this work, we report the synthesis of nanocrystalline $CaWO_4$ and $NiWO_4$ powders from water-based citrate complex precursor using microwave irradiation. The precursors and powders were evaluated through their crystallization process and thermal decomposition processes and by identifying particle morphology.

2. Experimental

Metal nitrates ($Ca(NO_3)_2{\cdot}4H_2O$, $Ni(NO_3)_2{\cdot}6H_2O$, Junsei Chemical Co. Ltd., Japan) and ammonium tungstate ($(NH_4)_{10}W_{12}O_{41}{\cdot}5H_2O$, Junsei Chemical Co. Ltd., Japan) were used as the metallic cations. De-ionized water (DW) and citric acid ($HOC(CO_2H)(CH_2CO_2H)_2$, CA, Yukiri Pure Chemical Co. Ltd., Japan) were used as the solvent and chealating agent for the process. Fig. 1 shows the schematic flow chart for the synthesis of nano-sized $CaWO_4$ and $NiWO_4$ powders by the modified citrate complex method

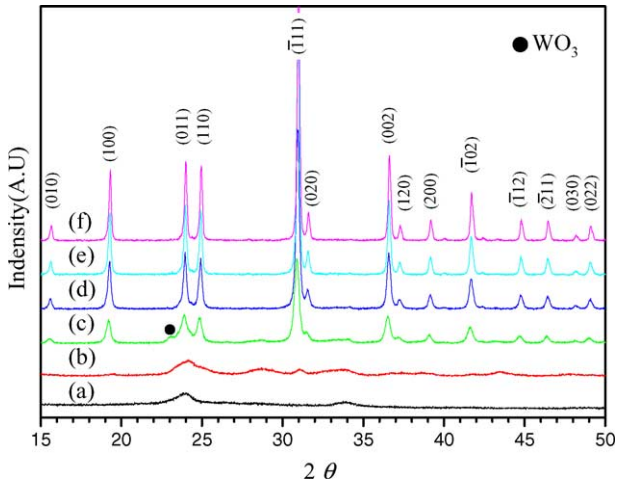

Fig. 2. XRD patterns of the $NiWO_4$ powders (a) precursor and heat-treated at (b) 300, (c) 350, (d) 400, (e) 450, (f) 500 °C for 3 h.

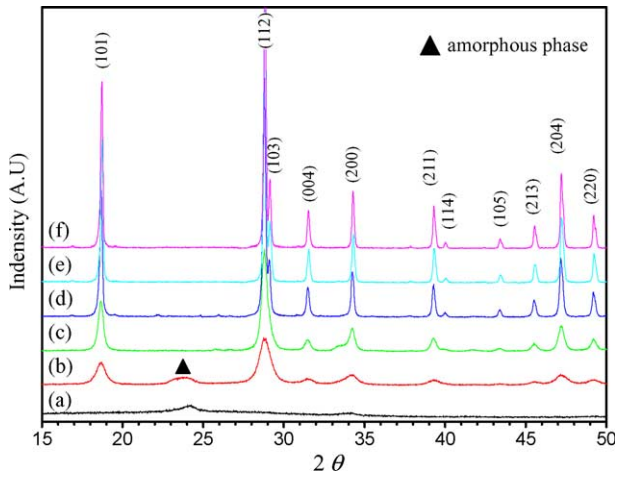

Fig. 3. XRD patterns of the $CaWO_4$ powders (a) precursor and heat-treated at (b) 300, (c) 350, (d) 400, (e) 450, (f) 500 °C for 3 h.

using microwave irradiation. The citrate solution was prepared by dissolving appropriate molar ratio of citric acid in de-ionized water (CA:DW molar ratio = 1:4). After complete homogenization of the citrate solution, metal nitrate and ammonium tungstate were dissolved in the molar ratio of total chelate metal cations (TO) and citric acid (TO:CA molar ratio = 1:5). By keeping the solution at a temperature of 100 °C for 1 h under constant stirring, the solution became viscous. A domestic microwave oven (Samsung Electronic Corp., Korea, 2.45 GHz, 1200 W) was conducted for the reactions in the solution. The solution was placed in the microwave oven and the reactions were performed under ambient air for 30 min. The microwave oven followed a working cycle of 40 s on and 20 s off. The solution became more viscous with time and changed its color to brown. No visible precipitation was observed during the heating process. As this solution condensed, the brown product was converted into powders after grinding with a Teflon bar. Thermal analysis was performed on this powder, hereinafter referred to as the 'precursor'. Heat-treatment of the precursor was performed at various temperatures from 300 to 500 °C for 3 h.

The crystallization process of the polymeric precursor was evaluated by thermogravimetry–differential thermal analysis (TG-DTA, SETRAM, France), using a sample weight of about 24 mg and a heating rate of 5 °C/min. The existing phase in the particles after heat-treatment was identified by ordinary X-ray diffraction (XRD, Cu Kα, 40 kV, 30 mA, Rigaku, Japan) with a scan rate of 3 °C/min. The microstructure and electronic diffraction patterns (EDP)

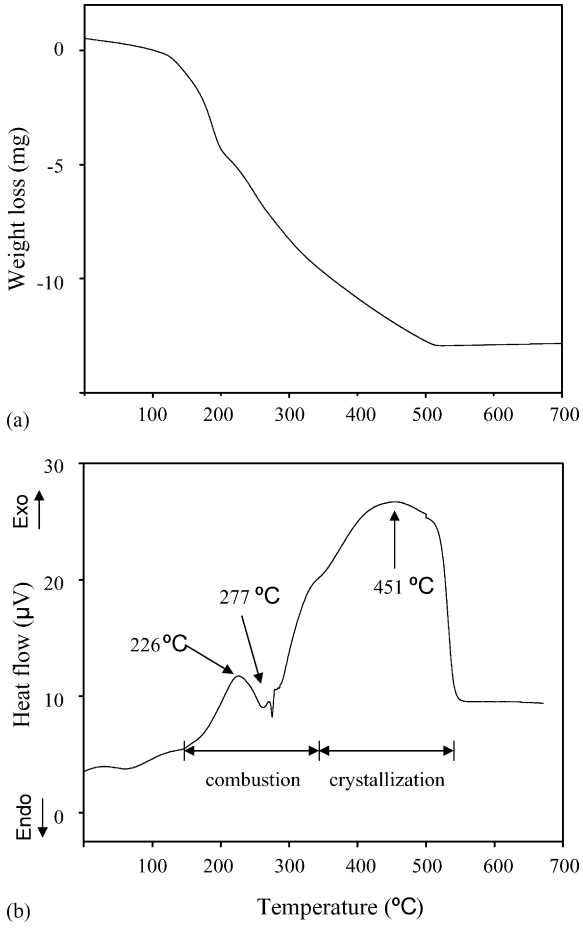

Fig. 4. (a) TGA and (b) DTA curves of the $NiWO_4$ precursors in flowing air.

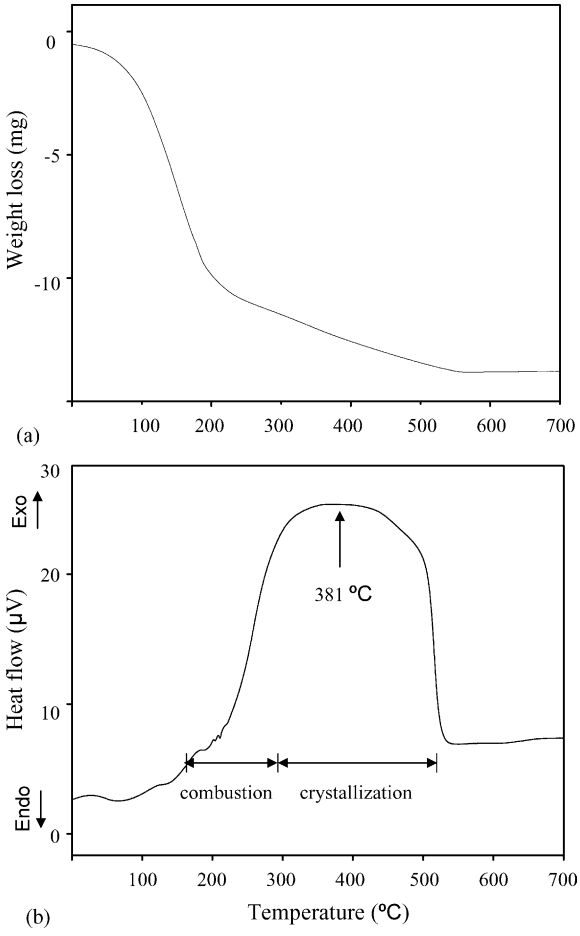

Fig. 5. (a) TGA and (b) DTA curves of the $CaWO_4$ precursors in flowing air.

of the particles were observed by transmission electron microscopy (TEM, JEM 2010). The average crystallite size of the heat-treated particles was calculated by using the X-ray diffractometry line broadening method through the Scherrer's relationship [22].

3. Results and discussion

Figs. 2 and 3 show the phase identification of the $NiWO_4$ and $CaWO_4$ particles heated for 3 h as a function of heating temperature in detail using XRD. In Fig. 2(a) and (b), the precursor and powders of $NiWO_4$ at 300 °C were amorphous without any crystallized phases. Above 350 °C in Fig. 2(c) and (f), the particles could be identified as the $NiWO_4$ phase. At 350 °C in Fig. 2(c), unreacted WO_3 phase was observed and it seemed to be an additional phase to the $NiWO_4$ phase. For a higher heating temperature, at 400 °C in Fig. 2(d), the WO_3 peaks disappeared and the $NiWO_4$ peaks showed higher intensity. Fig. 3 shows the phase formation of $CaWO_4$ beginning at lower temperatures as compared to the case of $NiWO_4$. In Fig. 3(a), the $CaWO_4$ precursor was amorphous without any crystallized phases. Above 300 °C in Fig. 3(b), the particles could be identified as $CaWO_4$ phases. However, at 300 °C in Fig. 3(b), amorphous phase was observed. For a higher heating temperature, above 350 °C in Fig. 3(c), the amorphous phase disappeared and only $CaWO_4$ peaks showed up.

Figs. 4 and 5 show the TG-DTA curves for the $NiWO_4$ and $CaWO_4$ precursor, respectively. In Fig. 4(a), with the increase of temperature, the weight loss of the $NiWO_4$ precursor occurs in the TG curve up to 500 °C. Thereafter the weight remains constant, indicating that the decomposition of all organic materials and the crystallization have been completed below 500 °C. No significant plateau, corresponding to well-defined intermediate products, appeared in the heating process. The DTA curve in Fig. 4(b) shows three exothermic peaks which could be further classified into two types of physical meaning: (1) left exothermic peak at 226 °C corresponds to the initial decomposition of the precursor; (2) center exothermic peak at 277 °C; (3) right exothermic peak at 451 °C correspond to the formation of the nucleus of the crystal and crystallization of $NiWO_4$. In Fig. 5(a), with the increase of temperature, the weight loss of $CaWO_4$ precursor occurs in the TG curve up to 520 °C. The DTA curve of $CaWO_4$ precursor shows some difference with the case of $NiWO_4$. Weight loss curve of $CaWO_4$ precursor in a temperature range to 250 °C is steeper than that of $NiWO_4$ precursor. The DTA curve in Fig. 5(b) shows two peaks composed of a weak exothermic peak at

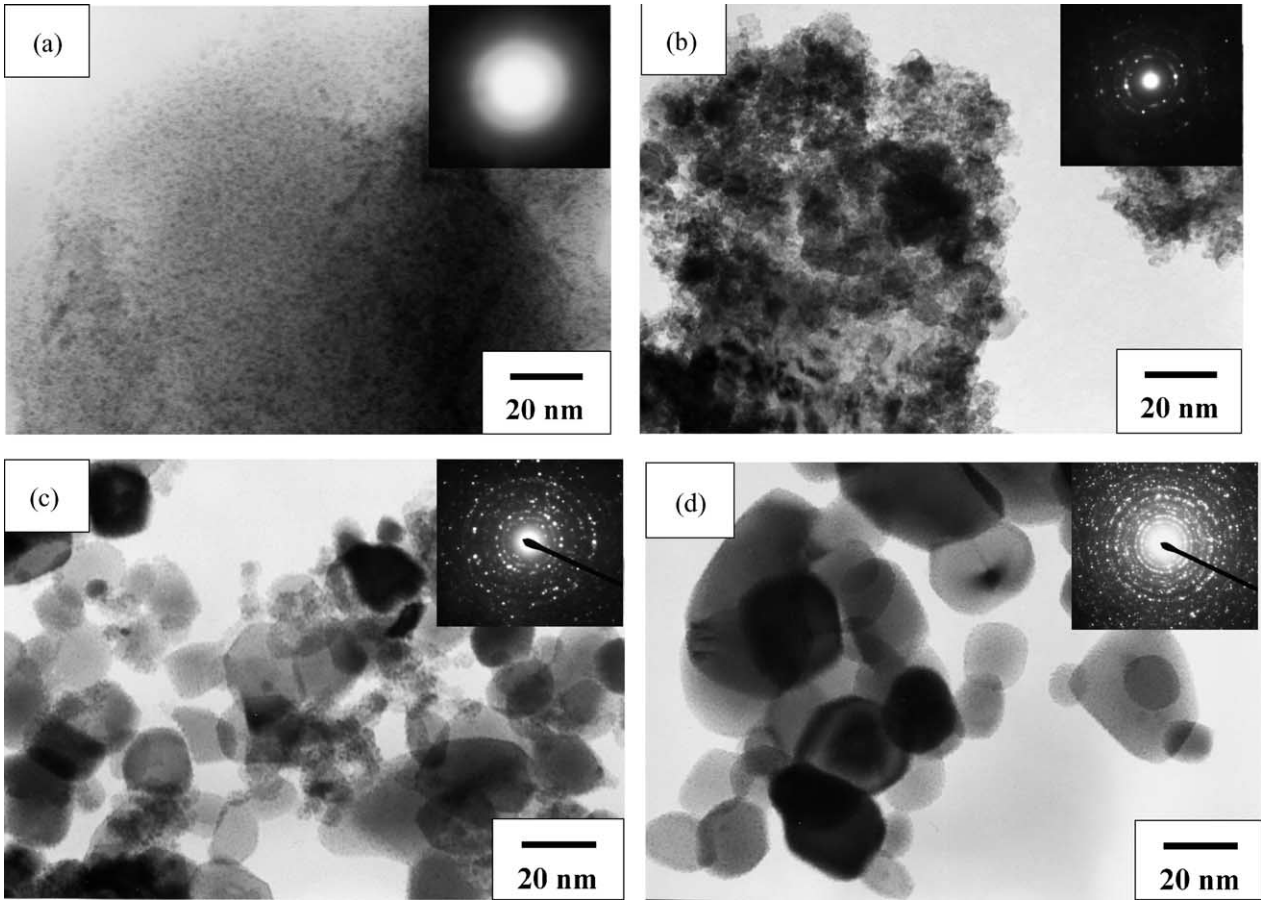

Fig. 6. TEM and EDP of nano-sized $NiWO_4$ powders heat-treated at (a) 300, (b) 350, (c) 400 and (d) 450 °C for 3 h.

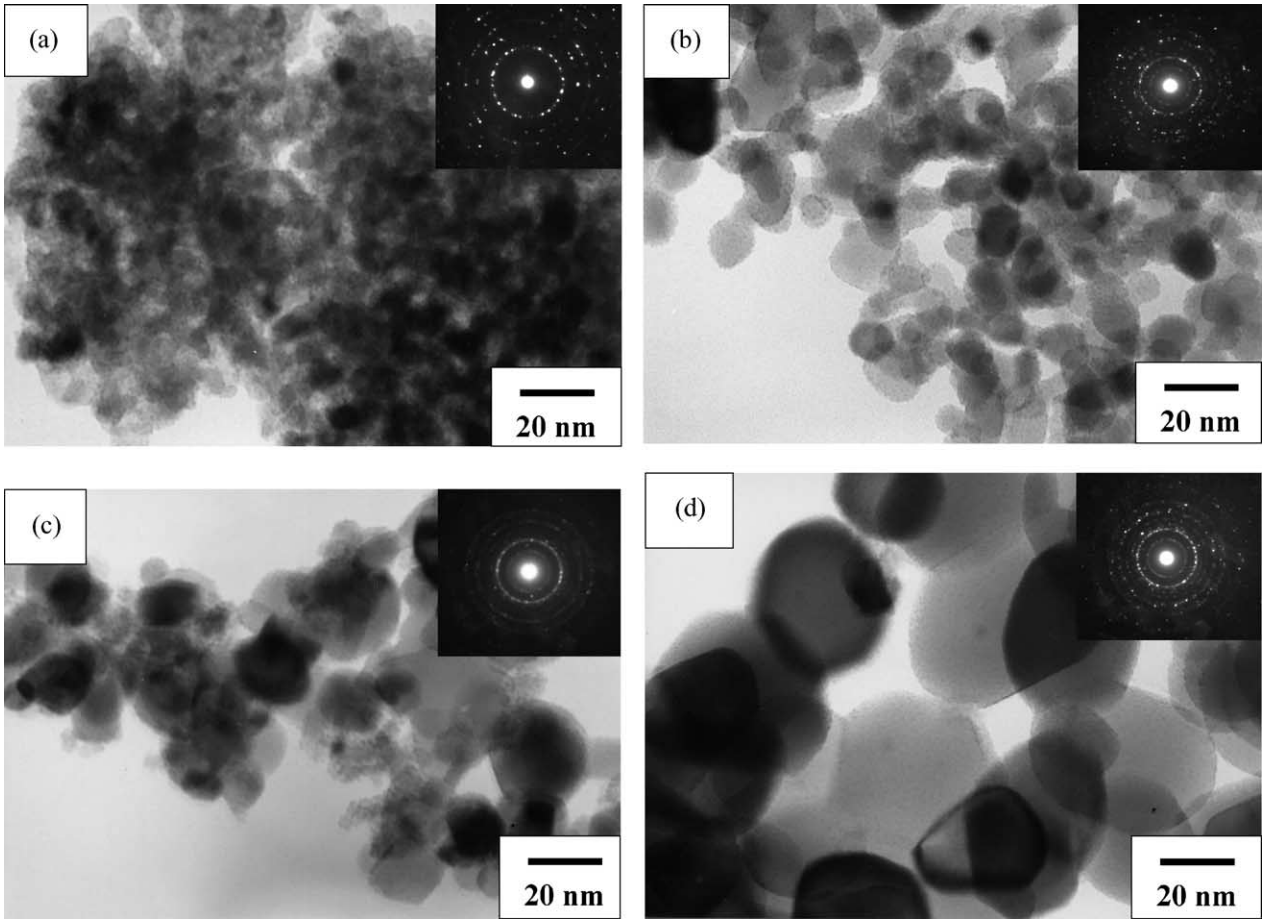

Fig. 7. TEM and EDP of nano-sized $CaWO_4$ powders heat-treated at (a) 300, (b) 350, (c) 400 and (d) 450 °C for 3 h.

210 °C and an exothermic range from 300 to 500 °C. These results indicate that $CaWO_4$ precursors begin to decompose from near 210 °C and phase formation proceeds subsequently from near 300 to 500 °C.

Figs. 6 and 7 show TEM and electronic diffraction pattern of the $NiWO_4$ and $CaWO_4$ powders prepared at different temperatures for 3 h. The EDP of $NiWO_4$ powders heat-treated at 300 °C in Fig. 6(a) showed only diffuse hollow rings, corresponding to an amorphous phase. With increasing temperature, at 350 °C in Fig. 6(b), dotted rings were observed, signifying the nanocrystallite (nuclei of crystals) formation. The initial crystallization temperature seemed to be at 350 °C, corresponding to the results of XRD and TG-DTA. The TEM morphology in Fig. 6(a) and (d) showed that the sizes of the crystallites gradually increased with the temperatures. The EDP of $CaWO_4$ powders in Fig. 7(a) showed the dotted ring patterns at a temperature of 300 °C. The initial crystallization temperature is 300 °C, which is lower than that of $NiWO_4$. Nano-powders of $CaWO_4$ and $NiWO_4$ heat-treated between 350 and 450 °C showed primarily spherical and homogeneous morphology. The $CaWO_4$ powders at 450 °C in Fig. 7 (d) showed some exaggerated growth accompanying by faceting of the crystals.

The average grain sizes were determined from XRD patterns according to the Scherrer's equation [22].

$$D = \frac{k\lambda}{\beta \cos\theta}$$

where D is the average grain size, k the constant equal to 0.89, λ the wavelength of X-rays equal to 0.1542 nm and β the corrected half-width that is obtained by using (1 1 1) line of the pure silicon as the standard. Table 1 shows the average crystallite sizes for the heat-treated powders calculated by XRD line broadening method. The calculated average crystallite sizes of $NiWO_4$ were 14, 20, 23 and 29 nm at temperatures of 350–500 °C, and the sizes of $CaWO_4$ were

Table 1
Calculated average crystallite size of $NiWO_4$ and $CaWO_4$ powders as a function of heating temperature

Temperature (°C)	Average crystallite size (nm)	
	$NiWO_4$	$CaWO_4$
300	–	12
350	14	15
400	20	21
450	23	27
500	29	35

12, 15, 21, 27 and 35 nm at temperatures of 300–500 °C. These correspond to the TEM observation as shown in Figs. 6 and 7 indicating an ordinary tendency of grain growth with temperature.

4. Conclusion

Nano-sized $CaWO_4$ and $NiWO_4$ powders were successfully synthesized by the modified citrate complex method under microwave irradiation. Crystallization of $CaWO_4$ and $NiWO_4$ particles were detected at 300 and 350 °C, respectively, and completed entirely at a temperature of 400 °C. Most of the $CaWO_4$ and $NiWO_4$ nanocrystalline powders heat-treated between 350 and 450 °C showed primarily spherical and homogeneous morphology. The average crystallite sizes of $CaWO_4$ were between 12 and 35 nm, and those for $NiWO_4$ were between 14 and 29 nm, showing an ordinary tendency to grow with the temperature.

References

[1] Z. Bryknar, R. Grasser, Z. Potucek, A. Scharmann, P. Bohacek, J. Lumine. 72 (1997) 643–645.
[2] L.F. Johnson, G.D. Boyd, K. Nassau, R.R. Soden, Phys. Rev. 126 (4) (1962) 1406–1409.
[3] H. Wang, F.D. Medina, Y.D. Zhou, Q.N. Zhang, Phys. Rev. B 45 (1992) 10356–10362.
[4] W. Carel, E. van Eijk, Nucl. Instrum. Methods Phys. Res., A 392 (1997) 285–290.
[5] R. Sundaram, K.S. Nagaraja, Mater. Res. Bull. 39 (2004) 581–590.
[6] B. Lake, D.A. Tennant, Physica B 234 (1997) 557–559.
[7] J. Tamaki, T. Fujii, K. Fujimori, N. Miura, N. Yamazoe, Sens. Actuators B 24 (1995) 396–399.
[8] S.H. Yu, B. Liu, M.S. Mo, J.H. Huang, X.M. Liu, Y.T. Qian, Adv. Funct. Mater. 13 (8) (2003) 639–647.
[9] R. Graser, E. Pitt, A. Scharmann, G. Zimmerer, Phys. Status Solidi B 69 (1975) 359–368.
[10] E.F. Paski, M.W. Blades, Anal. Chem. 60 (11) (1988) 1224–1230.
[11] A.R. Phani, M. Passacantando, L. Lozzi, S. Santucci, J. Mater. Sci. 35 (2000) 4879–4883.
[12] D. Chen, G. Shen, K. Tang, H. Zheng, Y. Qian, Mater. Res. Bull. 38 (2003) 1783–1789.
[13] K. Kuribayashi, M. Yoshimura, T. Ohta, T. Sata, Bull. Chem. Soc. Jpn. 50 (11) (1977) 2932–2934.
[14] M.P. Pechini, US Patent 3,330,697 (July 11, 1967).
[15] S. Kumar, G.L. Messing, W.B. White, J. Am. Ceram. Soc. 76 (1993) 617–624.
[16] M. Yoshimura, J. Ma, M. Kakihana, J. Am. Ceram. Soc. 81 (1998) 2721–2724.
[17] N.G. Eror, H.U. Anderson, Mater. Res. Soc. Symp. Proc. 73 (1986) 571–577.
[18] M. Kakihara, M. Yoshimura, H. Mazaki, H. Yasuoka, L. Borjesson, J. Appl. Phys. 71 (1992) 3904–3910.
[19] C. Jansen, A. Arafat, A.K. Barakat, H. Van Bekkum, in: M.L. Occelli, H. Robson (Eds.), Synthesis of Microporous Materials, vol. 1, Van Nostrand Reinhold, New York, 1992, pp. 507–508.
[20] T. Ohgushi, K. Ishimaru, J. Am. Ceram. Soc. 84 (2) (2001) 321–327.
[21] R. Roy, S. Komarneni, J.L. Yang, J. Am. Ceram. Soc. 68 (1985) 392–395.
[22] B.D. Cullity, Elements of X-ray Diffraction, second ed. Addison-Wesley Publishing Company Inc., MA, 1978, pp. 101–102.